Chemical Engineering Journal 162 (2010) 164–170

Contents lists available at ScienceDirect

Chemical Engineering Journal

journal homepage: www.elsevier.com/locate/cej

Removal of arsenic by a granular Fe–Ce oxide adsorbent: Fabrication conditions and performance

Yu Zhang[a,*], Xiaomin Dou[c,a], Bei Zhao[a], Min Yang[a,*], Tomoo Takayama[b], Shigeru Kato[b]

[a] State Key Laboratory of Environmental Aquatic Chemistry, Research Center for Eco-Environmental Sciences, Chinese Academy of Sciences, Beijing 100085, China
[b] Advanced Reactor Fuels Department, Japan Nuclear Fuel Industries, Ltd., Naka-gun, Ibaraki 319-1196, Japan
[c] College of Environmental Science and Engineering, Beijing Forestry University, 100083 Beijing, China

ARTICLE INFO

Article history:
Received 17 March 2010
Received in revised form 12 May 2010
Accepted 12 May 2010

Keywords:
Granular Fe–Ce oxide
Vibration dropping method
As(V) removal

ABSTRACT

Iron–cerium hydroxide (Fe–Ce), which has shown a high arsenic (V) (As(V)) adsorption capacity in previous studies, was granulated using the vibration dropping method used to prepare small-sized fuel particles. Fabrication studies showed that the sintering process could not be used in the preparation of the granular Fe–Ce (GFC) adsorbent and that the optimum grain size was 1.0 mm for As(V) removal. The optimum sized GFC (GFC-1.0 mm) exhibited a Freundlich adsorption of 18.2 and 11.8 mg g^{-1} at an equilibrium concentration of 1.0 and 0.1 mg L^{-1}, respectively. The GFC-1.0 mm also showed equivalent As removal performance to READ, a commercial adsorbent with CeO_2 as the sole metal oxide component (about 81%), under both space velocities of 240 and 24 h^{-1} in column tests. The cost for the manufacturing of GFC, however, is much lower since iron is the major metal component (about 80%). Energy dispersive X-ray microanalysis (EDX) results showed that As was distributed from the surface to the center of the GFC after the As(V) adsorption experiment, suggesting that nearly all active sites inside the GFC were available for the removal of As(V). The As(V) on the used GFC could be desorbed with an efficiency of 89% using 1.0 mol L^{-1} sodium hydroxide, and the GFC after desorption showed similar As adsorption performance with the fresh GFC. In conclusion, the GFC consisting of 80% Fe and 20% Ce exhibited As removal performance equivalent to the commercial adsorbent consisting only of Ce.

1. Introduction

Due to its toxicity and carcinogenicity, the wide occurrence of arsenic (As) in groundwater has long been of global concern [1–7]. It has been speculated that over 100 million people worldwide are exposed to high concentrations of As in drinking water [1,8], and significant effort has been devoted to solving this problem.

Among the different options proposed, adsorption has been considered the most cost-effective technology in relation to the removal of As from groundwater [8]. A wide range of low-cost adsorbents have been reported for As removal, including natural materials [9], synthetic activated carbons [10,11], agricultural and industrial products (or by-products and waste) [12–14], soil and constituents [15], and hydrotalcites [16]. However, these materials need frequent regeneration or replacement due to their relatively low adsorption capacities. Consequently, the development of As adsorbents with high adsorption capacities has been a primary goal of much scientific research, with some investigations already reporting that adsorbents such as zero-valent iron [17], single or mixed oxides [18], and metal-based resins [19,20] have high As adsorption capacity. Some adsorbents have also been successfully commercialized [8]. Among the commercial adsorbents, the adsorbent READ (URL http://www.asahi-kasei.co.jp/salt/), which uses hydrous cerium oxide as its major active component, has been used to remove As from industrial wastewater. While this material has a high adsorption capacity and can be regenerated easily, its high cost has limited its application in drinking water, particularly in the developing world. In addition, although interest in granular ferric hydroxide (GFH), another commercialized iron-based adsorbent, has grown due to its relatively low production costs, this material cannot be regenerated easily [8,21]. Consequently, its replacement cost is very high when it is applied to groundwater with relatively high As concentrations. In earlier studies, we successfully developed an iron–cerium (Fe–Ce) bimetal oxide, which exhibited an As(V) adsorption capacity significantly higher than many adsorbents previously reported [22,23]. Additionally, production costs can be reduced considerably due to the use of both Fe and Ce as the active components. The major challenge was, however, how to manufacture

---

* Corresponding authors. Tel.: +86 10 62923475; fax: +86 10 62923541.
E-mail addresses: zhangyu@rcees.ac.n (Y. Zhang), yangmin@rcees.ac.cn (M. Yang).

1385-8947/$ – see front matter © 2010 Elsevier B.V. All rights reserved.
doi:10.1016/j.cej.2010.05.021

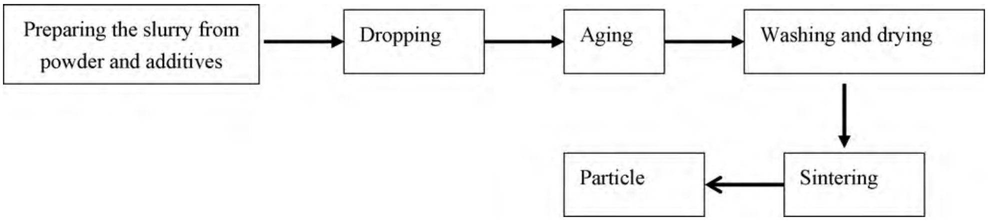

Fig. 1. Schematic diagram of the wet-gelation vibration dropping method.

a durable particle type adsorbent without sacrificing its adsorption capacity.

Coating and loading (or impregnating) active components to a carrier can be easily realized and has often been tried in the preparation of granular adsorbents [10,11,14,24–28]. These adsorbents, however, suffer from several drawbacks such as low adsorption capacity caused by limited active components, and low stability and durability [29]. Among several particle fabrication technologies reported [30–32], the vibration dropping method is considered an effective mechanism as it can fabricate homogeneous small-sized particles from powdered materials without a carrier core and has been successfully applied in the preparation of small-sized fuel particles on a mass production scale [32].

In the present study, a granular As adsorbent (GFC) was prepared from the Fe–Ce powder using the vibration dropping method, and its performance as well as some characteristics in the removal of As(V) was evaluated through comparison with several commercial materials.

2. Materials and methods

2.1. Preparation of adsorbent in powder and granule forms

The Fe–Ce bimetal oxide powder was prepared by a co-precipitation method [22,23]. Approximately 0.08 mol L^{-1} $Ce(SO_4)_2 \cdot 4H_2O$, 0.2 mol L^{-1} $FeCl_3 \cdot 6H_2O$, and 0.1 mol L^{-1} $FeCl_2 \cdot 4H_2O$ was dissolved together in distilled water. Under gentle stirring, the pH was slowly raised to around 10 by the addition of 6 mol L^{-1} NaOH solution. After 12 h of aging at room temperature, the suspension was repeatedly washed with distilled water and then dried at 100 °C for 10 h. The spherically shaped granular adsorbent, with different average diameters, was fabricated from the Fe–Ce bimetal oxide powder using a wet-gelation vibration dropping method [32] at Nuclear Fuel Industries, Ltd., Japan. The schematic diagram of the vibration dropping method is shown in Fig. 1 and the properties of the different GFCs are summarized in Table 1.

A particle type activated alumina (KHD, 1.4 mm average diameter) was obtained from the Sumitomo Chemical Co., Ltd. Japan. Granular Zr–Fe bimetal oxide adsorbent (SEVENTOL, 0.4–1.0 mm in diameter) was obtained from the Takeda Pharmaceutical Company Ltd., Japan. The READ, which is prepared by combining hydrous cerium oxide with a supporting polymer (0.7 mm average diameter), was provided by the Nihon Kaisui Co., Ltd., Japan.

2.2. Batch experiments for As(V) adsorption

A 1000 mg L^{-1} As(V) stock solution was prepared by dissolving 4.1653 g $Na_2HAsO_4 \cdot 7H_2O$ in 1 L of distilled water. The As(V) bearing solutions were prepared by diluting the stock solution to given concentrations with distilled water. All other reagents used were of analytical grade.

Given volumes of As(V) stock solution were added separately to seven conical flasks, with the final volume of each increased to 100 ml with distilled water. The test solution pH was adjusted to 5.0 with 0.05 mol L^{-1} HCl or NaOH. $H_2AsO_4^-$ is the main As(V) species at pH of 5.0 [8]. The flasks were then shaken at 160 rpm and kept at 25 °C for 48 h following the addition of the adsorbent. The solutions were then filtered with a 0.45 μm membrane filter for analysis. The final pH was recorded and the concentration of residual As(V) was analyzed on an atomic fluorescence spectrometer (HG-AFS-610, Beijing Raileigh Analytic Instrument Corporation, China). The adsorption isotherms were studied by varying the doses of adsorbent under a fixed As(V) concentration (10 mg L^{-1}). Isotherms were modeled using the Freundlich equation. Container adsorption tests were also carried out in order to give blank adsorption. The experiments were repeated three times and the data were averaged. And the detection limits (D.L.), standard deviation (S.D.), and replicability for As(V) analysis were 0.016 μg L^{-1}, 3.13, and <3%, respectively.

2.3. Column study

Three kinds of column tests were performed using the granular adsorbent. Firstly, a Perspex column (column A) with a diameter of 1.4 cm and height of 28 cm was used for evaluating the effect of drying or sintering temperature on As(V) removal (GFC-2 mm-25 °C: drying at 25 °C without sintering and GFC-2 mm-sintered: sintering at 1000 °C). The quantity of particles used weighed 20 g. The As bearing influent (As(V) concentration, 0.5 mg L^{-1}) was prepared by dissolving $Na_2HAsO_4 \cdot 7H_2O$ in tap water (Beijing). Because pH of groundwater is generally between 7 and 8, the tests were conducted under pH 7.0 and 8.0, respectively, with a space velocity (SV) of 10 h^{-1}. The main As(V) species around pH 7.0 and 8.0 are $H_2AsO_4^-$ and $HAsO_4^{2-}$, respectively. The speciation should be one

Table 1
Properties of different granular Fe–Ce adsorbents.

Name of granular adsorbents	Average diameter (mm)	Average sphericity	True density (g cm^{-3})	BET surface area (m^2 g^{-1})	Compression strength before failure (N)
GFC-2.0 mm-sintered	1.75	1.03	1.88	0.86	3.0
GFC-2.0 mm	2.0	1.03	1.42	114.4	37.6
GFC-1.5 mm	1.5	1.03	1.16	7.2	7.4
GFC-1.0 mm	1.0	1.04	1.30	20.8	5.5
GFC-0.6 mm	0.6	ND	2.30	3.0	ND

ND—not detected.

of the important factors affecting the As(V) removal efficiency [8]. The column effluents were collected at regular intervals of time and the As(V) concentration was measured. Metals in the effluents, including Fe and Ce, were analyzed using Inductively Coupled Plasma-Mass Spectrometry (ICP-MS, Plasma Quad 3, VG Corporation, UK).

Secondly, a smaller Perspex column (column B) with a diameter of 0.8 cm and height of 10 cm was used for identifying the effect of average grain diameter on As adsorption (GFC-2 mm-25 °C, GFC-1.5 mm, GFC-1 mm, and GFC-0.6 mm). The quantity of particles used weighed 1 g. The tests were conducted under the following conditions: pH, 7.0; As(V) concentration, 10 mg L^{-1}; SV, 240 h^{-1} (4 mL min^{-1}) and 24 h^{-1} (0.4 mL min^{-1}).

Thirdly, pilot column experimental equipment was constructed and installed in Jixiangzhuang Village, Houshayu Town, Beijing, China. The adsorption column was filled with the GFC-1 mm particles to investigate the equipment's performance in As removal through continuous operation under field conditions. The treatment process has been previously described in Dou et al. [33]. The pretreated water flowed gravitationally to the adsorption column (effective volume, 1 L; inner diameter, 6 cm; packing height, 8.85 cm) packed with GFC-1.0 mm adsorbent particles. The SV was 3 h^{-1}.

2.4. Desorption experiments

After column adsorption (adsorption amount, 8.2 mg g^{-1}), the GFC-1 mm was collected and air-dried for the desorption experiments. The desorption tests were carried out by shaking the As loaded adsorbents (1 g) in 50 mL NaOH solutions of different concentrations of 0.06, 0.3, and 1.0 mol L^{-1} for a period of 24 h, respectively. The As(V) concentrations in the desorption solutions were then analyzed. The regenerated GFCs were evaluated by using column B as described in Section 2.3.

2.5. Characterization of GFCs

The GFC particles were characterized using the following methods. The specific surface areas of the GFCs (0.5 g) were determined by the BET method using N_2 gas. The density of the particles (1 g) was measured by the mercury densitometry. The microstructure, with average grain diameter and porosity (50 particles), was observed by photographic analysis equipment. The compressive strength data and X-ray powder diffractometer (XRD) were provided by Japan Nuclear Fuel Industries, Ltd., Japan. The morphology of the GFCs was detected by using a 30 kV HITACHI S-3000N scanning electron microscopy (SEM). The deposition of metal species on the transverse section of the GFC-1 mm after column adsorption of As (after column test using column B) was observed using an energy dispersive X-ray (EDX) analytical spectrometer (EDAX Inc., USA) connected to a field emission.

3. Results and discussion

3.1. Effect of sintering on the performance of GFC

Sintering is a common process for particle fabrication using the vibration dropping method [32]. To identify the effect of sintering on the performance of GFC, the As adsorption performance of two GFC adsorbents (GFC-2.0 mm without sintering and GFC-2 mm-sintered at 1000 °C) was compared using column A (Fig. 2). For GFC-2.0 mm, the effluent As concentration reached the breakthrough point (As = 0.05 mg L^{-1}) at 42 and 468 bed volumes for pH 8.0 and 7.0, respectively. For GFC-2 mm-sintered, however, the As concentration at the first sampling point (bed volume of 5) was over the breakthrough point at pH 8.0. Fe–Ce adsorbs As mainly through the ligand exchange between the surface M–OH groups and arsenate [23]. So it is possible that most of the surface M–OH groups were destroyed during sintering. As such, sintering should not be applied to the fabrication of GFC.

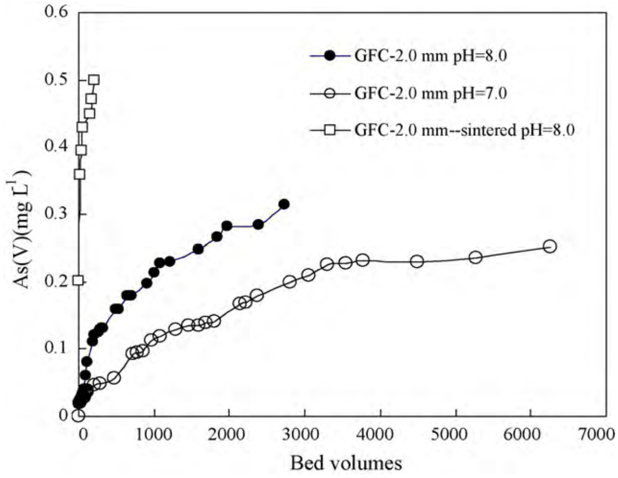

Fig. 2. Breakthrough curves for effect of particle fabrication temperature.

Fig. 3(a), (b), and (c) shows the XRD patterns of GFC-2.0 mm, GFC-2.0 mm-sintered, and Fe–Ce powder, respectively. Similar to the original Fe–Ce powder, the GFC-2.0 mm showed an amorphous structure, indicating that the process of wet-gelation vibration dropping had no obvious effect on the microcrystalline structure of the bimetal oxide. The XRD pattern of GFC-2.0 mm-sintered was, however, completely different. Obvious CeO_2 (JCPDS 43-4002) and Fe_2O_3 (JCPDS 33-0664) peaks were identified, showing that the sintering process had changed the structure of the material completely. At the same time, as can be seen from Table 1, the GFC-2.0 mm had a higher compression strength (37.6 N) and surface area (114.4 m^2 g^{-1}) than the GFC-2.0 mm-sintered (3.0 N and 0.86 m^2 g^{-1}). Additionally, the GFC-2.0 mm-sintered was gradually crushed into a fine powder after the column test. The high sintering temperature did decrease the physical strength, surface area, and pore volume, resulting in a decrease in the number of active sites and possibly explaining the reason for the different performances.

3.2. Effect of average grain diameters of GFCs and comparison with several commercial adsorbents on As(V) adsorption

Adsorbent grain size plays an important role in adsorption because it may affect the transportation rate of adsorbates inside the adsorbent particles and has a profound effect on the strength of particles by using the vibration dropping method [32]. The properties of different sized GFCs are compared in Table 1. It is clear that the fabrication processes with a decrease of particle size reduced the BET surface areas of the GFCs markedly, with GFC-0.6 mm showing the lowest one (3.0 m^2 g^{-1}). At the same time, the compression strength decreased with a decrease of particle size.

The As adsorption performance of different sized GFCs was evaluated by both batch and column experiments. The Freundlich isotherm model shown below was used to describe the batch adsorption behaviors of GFCs:

$$\log Q_{\mathrm{eq}} = \log k_{\mathrm{f}} + \frac{1}{n}\log C_{\mathrm{eq}}, \qquad (1)$$

where C_{eq} is the equilibrium concentration (mg L^{-1}), Q_{eq} is the amount adsorbed under equilibrium (mg g^{-1}), and k_{f} and n are empirical constants incorporating all factors affecting the adsorption process. The results, including the Freundlich isotherm equations as well as the standard deviation values, R^2, and the cal-

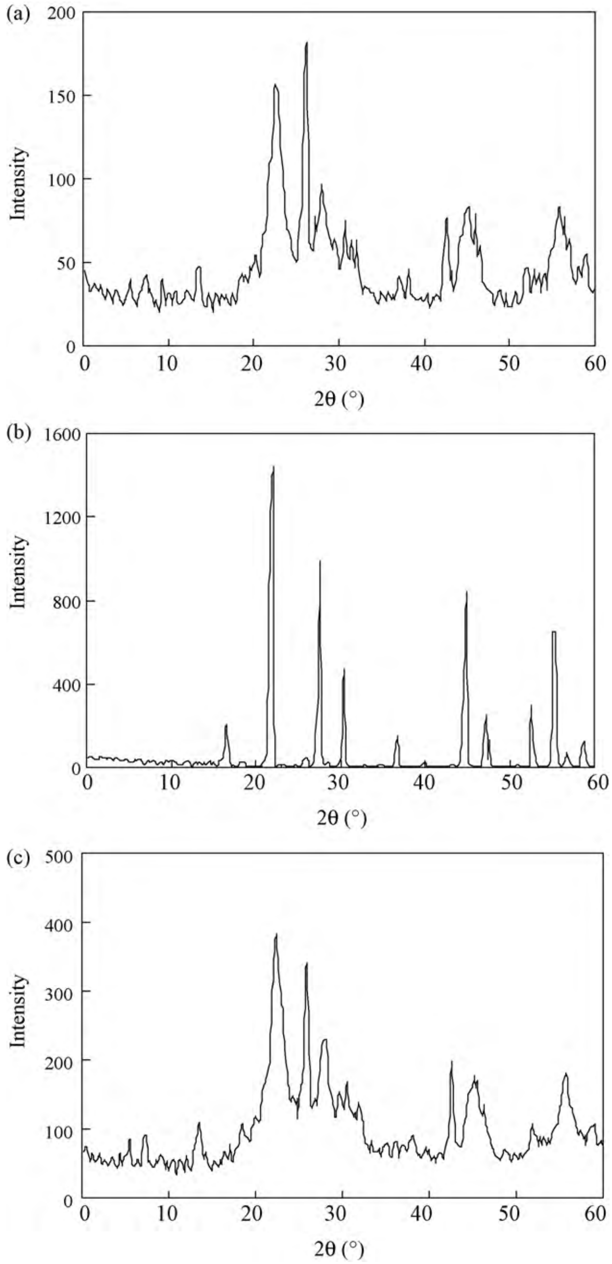

Fig. 3. XRD patterns of (a) GFC-2.0 mm, (b) GFC-2.0 mm-sintered, and (c) Fe–Ce powder.

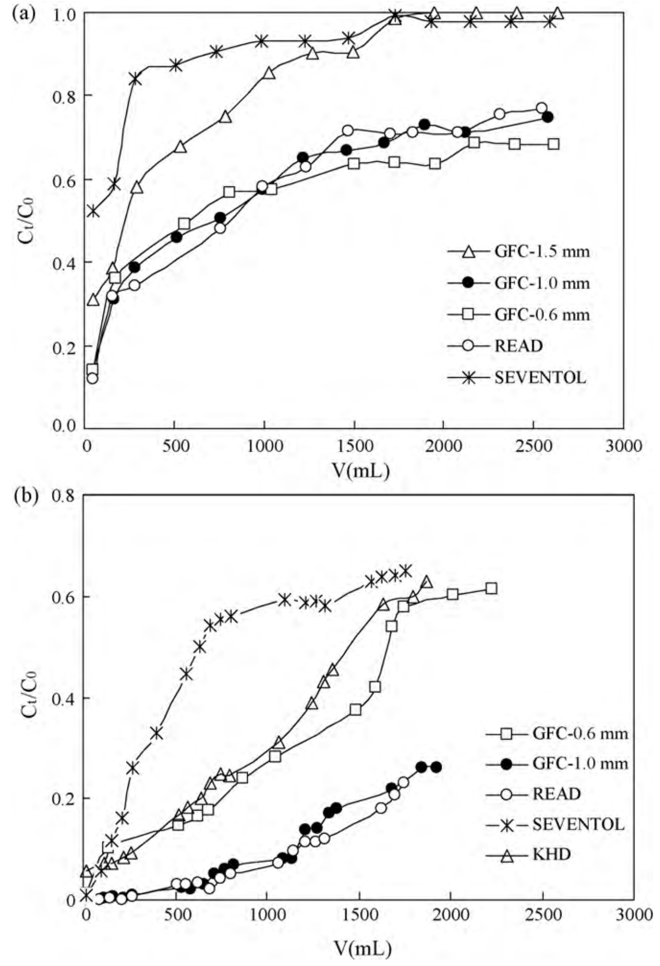

Fig. 4. Breakthrough curves of GFCs with different average grain diameters and several commercial adsorbents under SV (a) 240 h^{-1} and (b) 24 h^{-1}.

culated values of Q_{eq} under C_{eq} (0.1 and 1 mg L^{-1}), are listed in Table 2. Linear plots of ln Q_{eq} vs ln C_{eq} were obtained with R^2 and ranged from 0.81 to 0.99, showing that the Freundlich isotherm model was applicable for the As adsorption of GFCs. The calculated values of Q_{eq} for GFC-2.0 and GFC-1.5 mm were significantly lower than those for GFC-1.0 and GFC-0.6 mm under both low and high C_{eq} (Table 2). The smallest sized particle (GFC-0.6 mm) showed the highest calculated Q_{eq} under C_{eq} of 1.0 mg L^{-1}, while GFC-1.0 mm showed the highest Q_{eq} (11.78 mg g^{-1}) under C_{eq} of 0.1 mg L^{-1}. In addition, GFC-1.0 mm showed the similar calculated Q_{eq} under both low and high C_{eq} with READ.

The column tests (using column B) for GFC-1.5, GFC-1.0, and GFC-0.6 mm were conducted in comparison with several commercial adsorbents (KHD, SEVENTOL, and READ) under SVs of 240 and 24 h^{-1} at an influent As(V) of 10 mg L^{-1} at pH 7.0 (Fig. 4(a) and (b)). It is clear that GFC-1.0 and GFC-0.6 mm together with READ formed the high performance group under the high SV, while GFC-1.0 mm and READ formed the high performance group under the low SV. The GFC-1.0 mm showed equivalent As(V) removal performance to READ under different SV conditions, but was far more efficient than SEVENTOL and KHD. While READ has been shown to be effective for As removal in Japan, Bangladesh, and India (URL http://www.asahi-kasei.co.jp/salt/), its high cost due to the use of CeO_2 as its sole active component (about 81%) is a major drawback. For GFC, however, Fe

Table 2
Freundlich isotherm equations and calculated parameters for GFCs with different average grain diameters.

Granular adsorbents	GFC-2.0 mm	GFC-1.5 mm	GFC-1.0 mm	GFC-0.6 mm	READ
Average diameter (mm)	2.0	1.5	1.0	0.6	0.65-0.7
log k_f	0.93 ± 0.023	1.00 ± 0.051	1.26 ± 0.046	1.30 ± 0.021	1.26 ± 0.015
1/n	0.45 ± 0.012	0.50 ± 0.024	0.19 ± 0.018	0.46 ± 0.010	0.25 ± 0.019
R^2	0.99	0.81	0.91	0.93	0.98
Q_{eq} (mg g^{-1})(C_{eq} = 0.1 mg L^{-1})	3.0	3.2	11. 8	7.0	10.2
Q_{eq} (mg g^{-1}) (C_{eq} = 1 mg L^{-1})	8.6	10.1	18.2	20.1	18.1

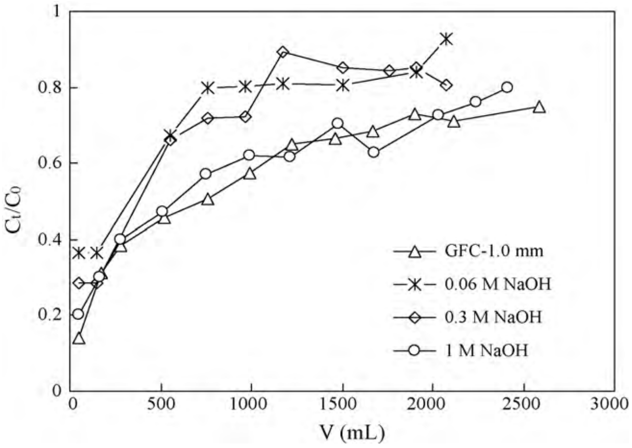

Fig. 5. Breakthrough curves of GFC and recycled GFC after regeneration.

can be used as a substitute for 80% of the Ce, which can significantly reduce the cost of the GFC.

As a granular adsorbent, it is usually expected that smaller adsorbent sizes have a higher removal capacity than bigger pieces [34]. Both Table 2 and Fig. 4 show, however, that GFC-0.6 mm was inferior to GFC-1.0 mm under low SV conditions and low equilibrium As concentration conditions, although there was a significant decrease in specific surface area (20.8–3.0 $m^2 g^{-1}$) with a decrease in particle size (1.0–0.6 mm) (Table 1). Conversely, if pellets or particles are exceedingly small, they may cause clogging problems in a packed-bed column and pressure loss [35]. Consequently, the diameter of 1.0 mm was considered the most reasonable particle size.

Table 3

Desorption of GFC after As(V) adsorption by different NaOH concentrations in 50 mL solutions (Adsorption capacity for As(V) 8.12 $mg g^{-1}$).

NaOH concentrations ($mol L^{-1}$)	0.06	0.3	1.0
Desorbed amount ($mg g^{-1}$)	0.98	5.43	7.24
Desorption efficiency (%)	12	67	89

In a previous pilot study, the GFC-1.0 mm particles were successfully applied for As removal from groundwater containing As of 70–100 $\mu g L^{-1}$ in a suburban area of Beijing [33]. Under an SV of 3 h^{-1} and pH 7.6 ± 0.2, the As(V) in effluent was kept lower than 10 $\mu g L^{-1}$ for approximately 150 days and 11,500 bed volumes. The cumulative adsorption amount of As(V) was 6.0 $mg g^{-1}$ media at the breaking point (effluent As(V) = 10 $\mu g L^{-1}$). This was higher than for porous granular ferric hydroxide (GFH, a commercial adsorbent) (breakthrough capacity 1.5 $mg g^{-1}$) in natural groundwater at pH 7.6–7.8 [36], $Al_2O_3/Fe(OH)_3$ (0.09 mg As g^{-1} at 50 $\mu g L^{-1}$) [37], zero-valent iron (4.4 mg As g^{-1} media) under an SV of 1.225 h^{-1} [38], and granular TiO_2 (1.7 $mg g^{-1}$, influent average As of 39 $\mu g L^{-1}$) [39]. As shown in Table S1, 18 metals (such as Fe, Ce, Cu, Zn, Cd, Cr, Mg, Al, and Mn ions), anions, and radioactivity in the effluent from the GFC column were analyzed during the column's operation. The results demonstrated the metal levels were under the MCL of WHO and China for drinking water or at the similar level as the influent (such as Ce). Radipactivity analysis of effluent showed that alpha and beta gross activities were 0.032 and 0.086 Bq L^{-1}, respectively, which were well below the proposed limit values of WHO and China (0.1 and 1.0 Bq L^{-1}).

3.3. Desorption and regeneration studies

While it is important for an adsorbent to possess a high adsorption capacity, the loaded adsorbates should also be able to be easily desorbed and reused on site. Sodium hydroxide (NaOH) solution has been utilized to regenerate As loaded adsorbents

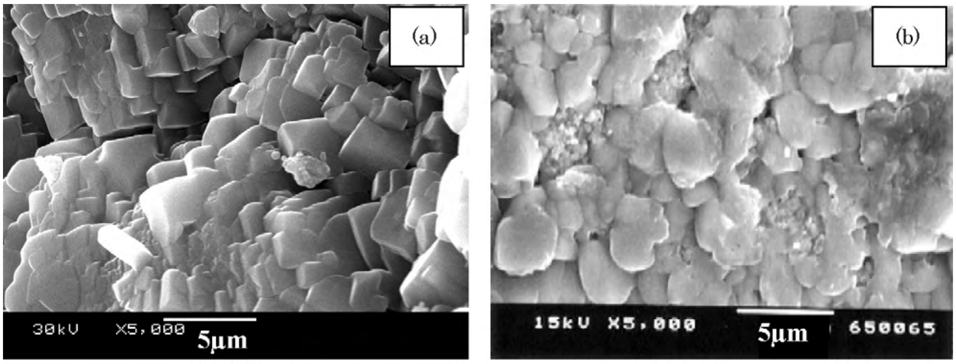

GFC-2.0 mm

GFC-1.5 mm

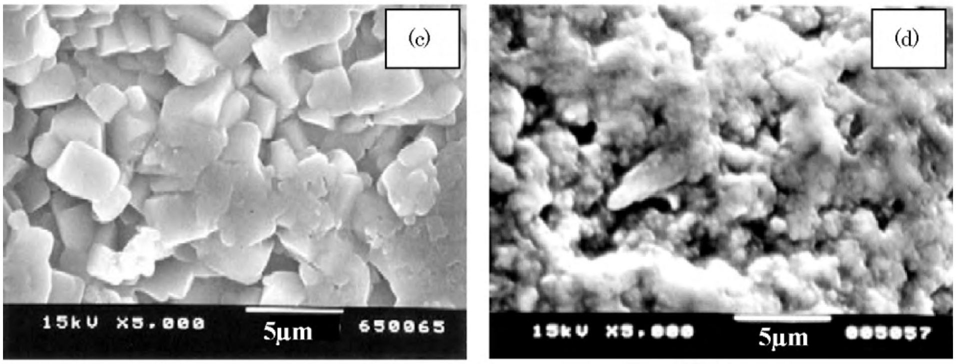

GFC-1.0 mm

GFC-0.6 mm

Fig. 6. SEM images of the GFCs with different average grain diameters: (a) GFC-2.0 mm, (b) 1.5 mm, (c) 1.0 mm, and (d) 0.6 mm (5000 times magnification).

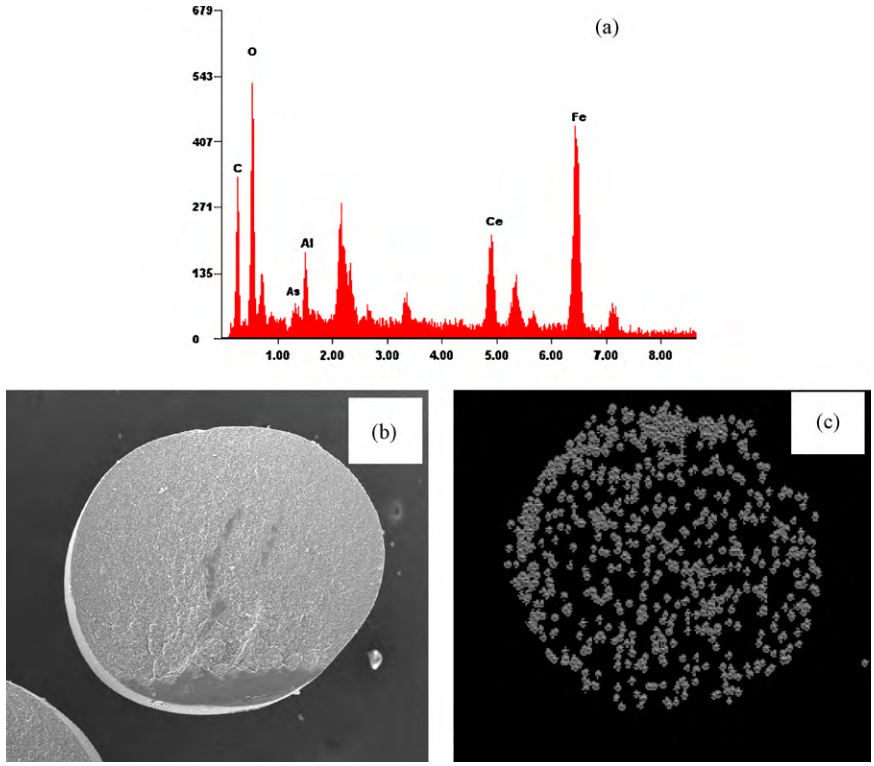

Fig. 7. The SEM/EDX results: (a) the elemental adequate spectra of GFC after As adsorption; (b) SEM image and (c) the mapping mode image of As in section plane of GFC after As adsorption (dot- As).

[15,25,40]. Desorption of As(V) from loaded GFCs (adsorption amount, 8.2 mg g^{-1}) was carried out under different NaOH concentrations (Table 3). While a NaOH concentration of 0.06 mol L^{-1} was found to be ineffective in the desorption of As(V) from the loaded GFC-1.0 mm, when the NaOH concentration was increased to 0.3 and 1.0 mol L^{-1} the desorption efficiency increased to 67 and 90%, respectively. The As(V) adsorption performance of the GFCs regenerated with different NaOH concentrations were evaluated by column tests (Fig. 5). It is clear that the GFC regenerated with 1 mol L^{-1} NaOH showed similar As(V) removal to the fresh GFC, demonstrating that an NaOH concentration of 1.0 mol L^{-1} was required for the efficient desorption of As(V) for GFC-1.0 mm. The minimum NaOH concentration for the efficient desorption of As(V) is determined by the adsorption capacities of the adsorbents. The desorption of As(V) from aluminum-coated Shirasu-zeolite has been successfully achieved with 40 mmol L^{-1} NaOH solution [40]. Bead cellulose loaded with iron oxyhydroxide has been regenerated when elution was carried out with 2 mol L^{-1} NaOH solution [25]. Although further studies are required, it is clear that the GFC-1.0 mm can be regenerated by NaOH and reused.

3.4. Distribution of As(V) inside GFC

The scanning electron microscopy (SEM) images (5000 times magnification) of the GFC-2.0, GFC-1.5, GFC-1.0, and GFC-0.6 mm particles are shown in Fig. 6(a), (b), (c), and (d), respectively. Relatively regular particles can be clearly identified for the GFC-2.0, GFC-1.5, and GFC-1.0 mm (Fig. 6(a), (b), and (c), respectively). Fig. 6(d), on the other hand, shows that the surface of GFC-0.6 mm was covered with small anomalous particles and therefore differed significantly from the other three particles.

To know whether the entire particle or just its surface was available for the adsorption of As(V), it is necessary to elucidate the distribution of As(V) inside the GFCs. The combination of SEM coupled with EDX can yield submicrometer scale, high quality elemental analysis [41], which has been utilized successfully for the direct detection of As dopant and distribution maps in semiconductor silicon devices [42], soil [43], and zero-valent iron [44]. The elemental distribution on the surface of GFC after As adsorption (using column B) was explored by a SEM combined with an EDAX KEVEX level 4. The EDX analysis revealed that Fe, Ce, and O were abundant on the surface and As was detected after column adsorption (Fig. 7(a)). In order to investigate the As distribution from the surface to the center of a particle, the mapping mode image of As in transverse section of a GFC after As adsorption was acquired as shown in Fig. 7(b) and (c) (before and after background deduction). It can be seen that As was distributed almost evenly across the transverse section, suggesting that nearly all of the active sites inside the GFC were available for the removal of As(V).

4. Conclusions

The Fe–Ce bimetal hydroxide adsorbent was fabricated by a wet-gelation vibration dropping method. The sintering process could not be applied for the preparation of the granular Fe–Ce adsorbent and the optimum grain size was 1.0 mm. The GFC consisting of 80% Fe and 20% Ce exhibited As removal performance equivalent to the commercial adsorbent consisting only of Ce, an important result as the material prepared in this study is much more cost-effective. Pilot column experiment under field conditions showed that the GFC-1.0 mm could remove As(V) from groundwater with high efficiency. As was found to be distributed from the surface to the center of the GFC after As(V) adsorption from EDX results, suggesting a high utilization efficiency of the active sites inside the GFC for adsorption. The GFC after desorption with NaOH showed similar As adsorption performance to the fresh GFC. The long time reuse of the adsorbent and the optimization of column operation parameters, however, require further study.

Acknowledgments

This work was supported by the National Natural Science Foundation of China (Nos. 50921064 and 50508006), the National High Technology Research and Development Program of China (2007AA06Z319), and Tianjin Special Innovation Fund (06FZZDSH00900). The authors are thankful to Dr. Christine J. Watts for providing language help.

Appendix A. Supplementary data

Supplementary data associated with this article can be found, in the online version, at doi:10.1016/j.cej.2010.05.021.

References

[1] P. Bagla, J. Kaiser, Epidemiology—India's spreading health crisis draws global arsenic experts, Science 274 (1996) 174–175.

[2] R.S. Burkel, R.C. Stoll, Naturally occurring arsenic in sandstone aquifer water supply wells of north-eastern Wisconsin, Ground Water Monit. Remediat. 19 (1999) 114–121.

[3] S.L. Chen, S.R. Dzeng, M.H. Yang, K.H. Chiu, G.M. Shieh, C.M. Wai, Arsenic species in groundwaters of the blackfoot disease area, Taiwan, Environ. Sci. Technol. 28 (1994) 877–881.

[4] X.J. Guo, Y. Fujino, S. Kaneko, K.G. Wu, Y.J. Xia, T. Yoshimura, Arsenic contamination of groundwater and prevalence of arsenical dermatosis in the Hetao plain area, Inner Mongolia, China, Mol. Cell. Biochem. 222 (2001) 137–140.

[5] I. Koch, J. Feldmann, L.X. Wang, P. Andrewes, K.J. Reimer, W.R. Cullen, Arsenic in the Meager Creek hot springs environment, British Columbia, Canada, Sci. Total Environ. 236 (1999) 101–117.

[6] M.F. Hossain, Arsenic contamination in Bangladesh—an overview, Agric. Ecosyst. Environ. 113 (2006) 1–16.

[7] P.L. Smedley, M. Zhang, G. Zhang, Z. Luo, Mobilisation of arsenic and other trace elements in fluviolacustrine aquifers of the Huhhot Basin, Inner Mongolia, Appl. Geochem. 18 (2003) 1453–1477.

[8] D. Mohan, C.U. Pittman, Arsenic removal from water/wastewater using adsorbents—a critical review, J. Hazard. Mater. 142 (2007) 1–53.

[9] M.P. Elizalde-Gonzalez, J. Mattusch, W.D. Einicke, R. Wennrich, Sorption on natural solids for arsenic removal, Chem. Eng. J. 81 (2001) 187–195.

[10] Z.M. Gu, J. Fang, B.L. Deng, Preparation and evaluation of GAC-based iron-containing adsorbents for arsenic removal, Environ. Sci. Technol. 39 (2005) 3833–3843.

[11] K.D. Hristovski, P.K. Westerhoff, T. Moller, P. Sylvester, Effect of synthesis conditions on nano-iron (hydr)oxide impregnated granulated activated carbon, Chem. Eng. J. 146 (2009) 237–243.

[12] H. Genc-Fuhrman, J.C. Tjell, D. McConchie, Adsorption of arsenic from water using activated neutralized red mud, Environ. Sci. Technol. 38 (2004) 2428–2434.

[13] S. Kundu, A.K. Gupta, Arsenic adsorption onto iron oxide-coated cement (IOCC): regression analysis of equilibrium data with several isotherm models and their optimization, Chem. Eng. J. 122 (2006) 93–106.

[14] S. Kundu, A.K. Gupta, As(III) removal from aqueous medium in fixed bed using iron oxide-coated cement (IOCC): experimental and modeling studies, Chem. Eng. J. 129 (2007) 123–131.

[15] H. Zhang, H.M. Selim, Kinetics of arsenate adsorption–desorption in soils, Environ. Sci. Technol. 39 (2005) 6101–6108.

[16] G.P. Gillman, A simple technology for arsenic removal from drinking water using hydrotalcite, Sci. Total Environ. 366 (2006) 926–931.

[17] R.D. Ludwig, D.J.A. Smyth, D.W. Blowes, L.E. Spink, R.T. Wilkin, D.G. Jewett, C.J. Weisener, Treatment of arsenic, heavy metals, and acidity using a mixed ZVI-compost PRB, Environ. Sci. Technol. 43 (2009) 1970–1976.

[18] A.M. Raichur, V. Panvekar, Removal of As(V) by adsorption onto mixed rare earth oxides, Sep. Sci. Technol. 37 (2002) 1095–1108.

[19] T.S. Anirudhan, M.R. Unnithan, Arsenic(V) removal from aqueous solutions using an anion exchanger derived from coconut coir pith and its recovery, Chemosphere 66 (2007) 60–66.

[20] M.J. Haron, M.Z.W. Yunus, M.A. Sukari, L.T. Wum, S. Tokugana, Removal of arsenic(V) by cerium(III) complexed chelating ion exchanger, Malays, J. Anal. Sci. 3 (1997) 193–204.

[21] W. Driehaus, Arsenic removal-experience with the GEH process in Germany, Water Supply 2 (2002) 275–280.

[22] Y. Zhang, M. Yang, X. Huang, Arsenic(V) removal with a Ce(IV)-doped iron oxide adsorbent, Chemosphere 51 (2003) 945–952.

[23] Y. Zhang, M. Yang, X.M. Dou, H. He, D.S. Wang, Arsenate adsorption on an Fe–Ce bimetal oxide adsorbent: role of surface properties, Environ. Sci. Technol. 39 (2005) 7246–7253.

[24] J.A. Munoz, A. Gonzalo, M. Valiente, Arsenic adsorption by Fe(III)-loaded open-celled cellulose sponge. Thermodynamic and selectivity aspects, Environ. Sci. Technol. 36 (2002) 3405–3411.

[25] X.J. Guo, F.H. Chen, Removal of arsenic by bead cellulose loaded with iron oxyhydroxide from groundwater, Environ. Sci. Technol. 39 (2005) 6808–6818.

[26] S.L. Lo, T.Y. Chen, Adsorption of Se(IV) and Se(VI) on an iron-coated sand from water, Chemosphere 35 (1997) 919–930.

[27] P. Mondal, C.B. Majumder, B. Mohanty, Effects of adsorbent dose, its particle size and initial arsenic concentration on the removal of arsenic, iron and manganese from simulated ground water by Fe^{3+} impregnated activated carbon, J. Hazard. Mater. 150 (2008) 695–702.

[28] H.-X. Wu, T.-J. Wang, X.-M. Dou, B. Zhao, L. Chen, Y. Jin, Spray coating of adsorbent with polymer latex on sand particles for fluoride removal in drinking water, Ind. Eng. Chem. Res. 47 (2008) 4697–4702.

[29] C.H. Lai, C.Y. Chen, B.L. Wei, S.H. Yeh, Cadmium adsorption on goethite-coated sand in the presence of humic acid, Water Res. 36 (2002) 4943–4950.

[30] O.M. Vatutsina, V.S. Soldatov, V.I. Sokolova, J. Johann, M. Bissen, A. Weissenbacher, A new hybrid (polymer/inorganic) fibrous sorbent for arsenic removal from drinking water, React. Funct. Polym. 67 (2007) 184–201.

[31] L. Zeng, A method for preparing silica-containing iron(III) oxide adsorbents for arsenic removal, Water Res. 37 (2003) 4351–4358.

[32] I. Minatsuki, M. Tanihira, Y. Mizokami, Y. Miyoshi, H. Hayakawa, F. Okamoto, I. Maekawa, K. Takeuchi, H. Kodama, M. Fukuie, N. Kan, S. Kato, K. Nishimura, T. Konishi, The role of Japan's industry in the HTTR design and its construction, Nucl. Eng. Des. 233 (2004) 377–390.

[33] X.M. Dou, Y. Zhang, M. Yang, Y.S. Pei, X. Huang, T. Takayama, S. Kato, Occurrence of arsenic in groundwater in the suburbs of Beijing and its removal using an iron–cerium bimetal oxide adsorbent, Water Qual. Res. J. Can. 41 (2006) 140–146.

[34] D.J. Jeon, S.H. Yeom, Recycling wasted biomaterial, crab shells, as an adsorbent for the removal of high concentration of phosphate, Bioresour. Technol. 100 (2009) 2646–2649.

[35] S.H. Yeom, K.Y. Jung, Recycling wasted scallop shell as an adsorbent for the removal of phosphate, J. Ind. Eng. Chem. 15 (2009) 40–44.

[36] P. Westerhoff, D. Highfield, M. Badruzzaman, Y. Yoon, Rapid small-scale column tests for arsenate removal in iron oxide packed bed columns, J. Environ. Eng. 131 (2005) 262–271.

[37] M. Hodi, K. Polyak, J. Hlavay, Removal of pollutants from drinking-water by combined ion-exchange and adsorption methods, Environ. Int. 21 (1995) 325–331.

[38] N.P. Nikolaidis, G.M. Dobbs, J.A. Lackovic, Arsenic removal by zero-valent iron: field, laboratory and modeling studies, Water Res. 37 (2003) 1417–1425.

[39] S Bang, M. Patel, L. Lippincott, X.G. Meng, Removal of arsenic from groundwater by granular titanium dioxide adsorbent, Chemosphere 60 (2005) 389–397.

[40] Y.H. Xu, T. Nakajima, A. Ohki, Adsorption and removal of arsenic(V) from drinking water by aluminum-loaded Shirasu-zeolite, J. Hazard. Mater. 92 (2002) 275–287.

[41] A. Worobiec, S. Potgieter-Vermaak, A. Brooker, L. Darchuk, E. Stefaniak, R. Van Grieken, Interfaced, SEM/EDX and micro-Raman spectrometry for characterisation of heterogeneous environmental particles—fundamental and practical challenges, Microchem. J. 94 (2010) 65–72.

[42] G. Servanton, R. Pantel, Arsenic dopant mapping in state-of-the-art semiconductor devices using electron energy-loss spectroscopy, Micron 41 (2010) 118–122.

[43] D.H. Moon, M. Wazne, I.H. Yoon, D.G. Grubb, Assessment of cement kiln dust (CKD) for stabilization/solidification (S/S) of arsenic contaminated soils, J. Hazard. Mater. 159 (2008) 512–518.

[44] K. Sasaki, H. Nakano, W. Wilopo, Y. Miura, T. Hirajima, Sorption and speciation of arsenic by zero-valent iron, Colloids Surf. A 347 (2009) 8–17.